Computers in Biology and Medicine 139 (2021) 105013

Contents lists available at ScienceDirect

Computers in Biology and Medicine

journal homepage: www.elsevier.com/locate/compbiomed

Integro-differential approach for modeling the COVID-19 dynamics - Impact of confinement measures in Italy

Francesco Salvadore [a], Giulia Fiscon [b,c,*], Paola Paci [b,c]

[a] CINECA, HPC Department, Rome Office, Italy
[b] Institute for Systems Analysis and Computer Science "Antonio Ruberti", National Research Council, Rome, Italy
[c] Department of Computer, Control and Management Engineering "A. Ruberti" (DIAG), Sapienza University of Rome, Rome, Italy

ARTICLE INFO

Keywords:
COVID-19
Mathematical modelling
SARS-CoV-2

ABSTRACT

The COVID-19 pandemic has overwhelmed the life and security of most of the world countries, and especially of the Western countries, without similar experiences in the recent past. In a first phase, the response of health systems and governments was disorganized, but then incisive, also driven by the fear of a new and dramatic phenomenon. In the second phase, several governments, including Italy, accepted the doctrine of "coexistence with the virus" by putting into practice a series of containment measures aimed at limiting the dramatic sanitary consequences while not jeopardizing the economic and social stability of the country. Here, we present a new mathematical approach to modeling the COVID-19 dynamics that accounts for typical evolution parameters (i.e., virus variants, vaccinations, containment measurements). Reproducing the COVID-19 epidemic spread is an extremely challenging task due to the low reliability of the available data, the lack of recurrent patterns, and the considerable amount and variability of the involved parameters. However, the adoption of fairly uniform criteria among the Italian regions enabled to test and optimize the model in various conditions leading to robust and interesting results. Although the regional variability is quite large and difficult to predict, we have retrospectively obtained reliable indications on which measures were the most appropriate to limit the transmissibility coefficients within detectable ranges for all the regions. To complicate matters further, the rapid spread of the English variant has upset contexts where the propagation of contagion was close to equilibrium conditions, decreeing success or failure of a certain measure. Finally, we assessed the effectiveness of the zone assignment criteria, highlighting how the reactivity of the measures plays a fundamental role in limiting the spread of the infection and thus the total number of deaths, the most important factor in assessing the success of epidemic management.

1. Introduction

The COVID-19 pandemic has meant a dramatic novelty for many countries not only in terms of health management but even with respect to the understanding of the phenomenon in progress, especially in those countries, as the European ones, not used to dealing with a large-scale epidemic in the recent past [1–5]. A crucial point for tracing and forecasting COVID-19 pandemic is related to the available epidemiological data [6,7]. In particular, we can summarize the problems related to COVID-19 data analysis into three main categories: (i) inaccuracy of epidemic data measurements (e.g., the number of infections or of healed individuals), mostly linked to the presence of asymptomatic infections [6,8–12]; (ii) lack of reproducible data extracted under similar conditions [6]; (iii) a poor understanding of parameters' effects. Some parameters are intrinsically hard to quantify as inputs (e.g., confinement measures or variants diffusion), but at least there are clear indications they have a significant effect in the epidemic dynamics; whereas the effect of other parameters is uncertain (e.g., the seasonal effect or the effect of the interruption of specific activities), or more elusive even to be defined (e.g., social habits) [13].

In this context, developing models capable of replicating past epidemiological trends – or even more ambitiously able to predict future trends – is extremely challenging. Among simpler models for studying the dynamics of an infective epidemic, the Kermack-McKendirck one [14] provided the basis for a variety of widespread deterministic compartmental models, known as SIR (Susceptible-Infected-Recovered)

* Corresponding author. Department of Computer, Control and Management Engineering "A. Ruberti" (DIAG), Sapienza University of Rome, Rome, Italy.
E-mail address: giulia.fiscon@iasi.cnr.it (G. Fiscon).

https://doi.org/10.1016/j.compbiomed.2021.105013
Received 27 July 2021; Received in revised form 30 October 2021; Accepted 31 October 2021
Available online 2 November 2021

models, consisting of a set of ordinary differential equations where control parameters are time-independent. Several models for tracing and forecasting COVID-19 epidemic are based on SIR-type models [15–22] or to their extension at different level of complexity in the number of considered variables [6,23–28]. In our previous work [6], we applied an extension of the SIR compartmental model that explicitly considers asymptomatic infectives, while disregarding the effect of containment measures. Wang et al. [25] extended the standard SIR model by incorporating time-varying isolation measures (e.g., government-level macro isolation and community-level micro inspection measures), while it does not consider the existence of asymptomatic subjects and of a period of incubation of the virus. Giordano et al. [26] proposed another extension of SIR-type model that discriminates between diagnosed (asymptomatic detected) and non-diagnosed (asymptomatic undetected) individual and on the severity of their symptoms (SOI), but disregards for a possible latency between exposure to the virus and onset of infectiousness. Other authors (Hao et al., 2020 [28] and Bhaduri et al. [27]) proposed a Susceptible, Exposed, Infected and Removed (SEIR) compartments model that can be more suitable to include the presence of a long incubation period [29] and to explicitly consider also the exposed compartment. However, the deterministic nature of SIR-type model leads to a series of limits, including an intrinsic rigidity of the simulated time dynamics, which become of great importance when we want to include the effects of variability over time of the conditions in which the epidemic occurs, such as the effect of any containment measures adopted by the governments during the pandemic. In this context, Flaxman et al., 2020 [30] implemented a Bayesian semi-mechanistic models that links the infection cycle to the observed deaths, aiming to evaluate the effect of non-pharmaceutical interventions on different European countries. A further attempt to explicitly correlate confinement measures with contagion outcomes was attempted in Santamaria et al. [31] and applied in European and Italian contexts. Notwithstanding the success of these approaches [30,31], they fail in not considering other important factors such as the effect of vaccination or the effect of the virus variant, affecting the resulting estimated data especially for longer-term modelling.

Here, we present an integro-differential model that considers: (i) the delay effects of the contagion due to the incubation period of the virus; (ii) the effects of the decrease in the population of susceptible due to the increase in the number of recovered from the virus; (iii) the effects of vaccination (albeit in the initial phase); (iv) the effects of the spread of the English variant, more contagious than the original non-mutated virus; and (v) the effects of confinement measurements. The latter was modeled through a parameter that we assumed to be chosen among 7 different values representing the macro-category of imposed confinement level, temporally set according to the ordinances of the Italian Ministry of Health [32]. In the adopted model and under appropriate assumptions, these values can be interpreted as estimates of the ideal basic reproduction number associated with each level of confinement. Thus, the purpose of this work is to understand the effect of the different confinement measures implemented in various Italian regions since the beginning of the pandemic, by extracting indicative values of this parameter, in order to have quantitative estimates of the effects of the adopted measures and to assess which strategies were more effective for the management of the epidemic trend. For evaluating our model, the Italian situation during the so called second wave is a significant test case since a strategic plan with scenarios differentiated on a regional basis was put in place, with confinement levels and attribution criteria quite uniform across the Italian regions.

2. Material and methods

2.1. The model

In a simplified scenario, we consider $c(t)$ as the number of daily infections at time t. Hereafter, we will refer $c(t)$ as the number of daily infections multiplied by one million and normalized with the population considered. In this way, comparisons between areas of different populations can be made with less effort. Following an approach similar to that used to derive the Volterra-Lotka equation [33,34], the trend of $c(t)$ can be modeled as the sum of the infections occurred at time $t-a$ multiplied by the transmissibility $\tau(a)$ of the individual at an infection age (i.e., time from infection) equal to a:

$$c(t) = \int_0^\infty c(t-a)\,\tau(a)\,da \tag{1}$$

Therefore, the total number of infected by a single individual, that is the *basic reproduction number* R_0 , corresponds to:

$$R_0 = \int_0^\infty \tau(a)\,da \tag{2}$$

If R_0 is less than 1, the epidemic tends to disappear while otherwise an exponential growth is expected.

equation (1) for $c(t)$ can become an evolutionary equation if it is assumed that the transmissibility is different from zero only from a minimum time (incubation) a_1 up to a maximum time (exhaustion of the infection) a_2.

$$c(t) = \int_{a_1}^{a_2} c(t-a)\,\tau(a)\,da \tag{3}$$

We set $a_1 = 5$ and $a_2 = 16$ in reasonable accordance with the typical infective range reported in literature [35].

In order to explicitly consider the pandemic evolution and the environmental conditions, we have to include a temporal dependency for the transmissibility, i.e.:

$$\tau(a,\ t) = \tau_{BASE}(a)\cdot F(t-a) \tag{4}$$

where $\tau_{BASE}(a)$ is the baseline transmissibility while $F(t-a)$takes into account the evolving environmental conditions. We assume a constant behavior for $\tau_{BASE} = \overline{\tau}$, while the function $F(t-a)$can be expressed as the composition (multiplication) of the different environmental conditions, i.e.:

$$F(t-a) = F_S(t-a)\cdot F_V(t-a)\cdot F_C(t-a) \tag{5}$$

with F_s the fraction of susceptible number on the total population, F_V a contagiousness factor related to the active virus variants, F_C a factor that depends on the implemented containment measure.

Thus, the evolution formula for daily infections given by equation (3) becomes:

$$c(t) = \overline{\tau}\int_{a_1}^{a_2} c(t-a)\,F_S(t-a)\,F_V(t-a)\,F_C(t-a)\,da \tag{6}$$

Without loss of generality, we can rescale (one of) the environmental factors to ensure that $\overline{\tau} = 1/(a_2 - a_1)$, thus equation (6) becomes:

$$c(t) = \frac{1}{a_2-a_1}\int_{a_1}^{a_2} c(t-a)\,F_S(t-a)\,F_V(t-a)\,F_C(t-a)\,da \tag{7}$$

equation (7) represents our modelling of the evolution of the number of daily infections $c(t)$ over the time, with the basic reproduction number R_0 given by.

$$R_0 = \frac{1}{a_2-a_1}\int_{a_1}^{a_2} F_S(t-a)\,F_V(t-a)\,F_C(t-a)\,da \tag{8}$$

Thus, in the ideal conditions in which no virus variant is diffused and that the number of susceptible individuals corresponds to the entire

population (i.e., $F_S = F_V = 1$), F_C assumes the meaning of ideal basic reproduction number R_0 at the different containment levels adopted. Thus, values of $F_C$greater than 1 mean the epidemic outbreaks, while values below unity indicate that the epidemics is under control.

By defining the reproduction number $R(t)$ at a certain time t as:

$$R(t) = F_S(t) \cdot F_V(t) \cdot F_C(t) \quad (9)$$

equation (8) becomes:

$$R_0 = \frac{1}{a_2 - a_1} \int_{a_1}^{a_2} R(t-a)\, da \quad (10)$$

In the following, the description of each term of equation (9) along with their parametrization is provided.

2.2. Susceptible number

We assumed in our model that the susceptible population (i.e., those who have not yet encountered the virus) decreases over the time as the number of infected and/or vaccinated people increases. Thus, it can be evaluated as the total population minus the number of total infections up to time t and minus a factor that consider the effect of the vaccination campaign. Then, normalizing the susceptible population with respect to the entire population N_P, the first environmental factor F_s can be expressed as:

$$F_S(t) = \frac{N_P - \int_0^t c(a)\, da - f_{VT} \cdot V(t - \delta_V)}{N_P} \quad (11)$$

where $V(t-\delta_V)$ is a function describing the number of vaccinated people over time obtained from official data (see Supplementary File) and we set $\delta_V = 20$[36], considering the vaccination to be effective 20 days after receiving the first dose; f_{VT} is the fraction of the vaccinated people which are actually protected from infection, which we roughly assumed equal to 75% for the vaccines currently used in Italy.

2.3. Virus variants

Among the variations of Sars-CoV-2, lineage B.1.1.7 – so-called "English variant" or "Kent variant" [37] – has assumed particular importance, during the second wave, due to its greater contagiousness, thanks to which it has become, also in Italy, clearly dominant within a few months. The investigations of the Italian Istituto Superiore di Sanità (ISS) evaluated the prevalence P_V of this variant on a regional scale at some time stations and showed how the diffusion of the variant occurred at significantly different speeds and time ranges between the different Italian regions (see table in Supplementary Fig. 1) [38,39]. By linearly interpolating the prevalence over time, it is then possible to model the contagiousness increase factor due to the diffusion of the variant for each region as the weighted average between non-mutated virus contagiousness (taken as unitary) and variant counterpart (Supplementary File -Supplementary Fig. 1):

$$F_V(t) = C_V P_V(t) + [1 - P_V(t)] \quad (12)$$

where C_V is the contagiousness of the lineage virus B.1.1.7 compared to the non-mutated one. The value of $C_V$is still difficult to quantify [40] and we decided to use a value 1.4 close to the results of ISS investigations [41]. A similar approach is also valid in the presence of more than two variants as long as the respective prevalence and infectiousness factors are known.

2.4. Containment measures

In order to estimate F_C, we parameterized the different Italian containment measures implemented on a national or regional scale in 7 classes corresponding to different values of F_C. Thus, we modeled F_C as a sequence made up of 7 constant parameters, each corresponding to a containment level based on the ordinances of the Italian Ministry of Health. The 7 classes are the following (Fig. 1):

Free - No containment - before 2020-03-09 (national implementation)
Lockdown – "Full" containment - from 2020-03-09 to 2020-05-03 (national implementation)
Summer - No containment but restrictions on the social behavior - from 2020-05-04 to 2020-08-31 (national implementation)
Light – "Light" containment - from 2020-09-01 to 2020-11-05 (national implementation).
Yellow - Yellow zone – from 2020-11-05 (regional implementation)
Orange - Orange zone – from 2020-11-05 (regional implementation)
Red - Red zone – from 2020-11-05 (regional implementation)

For the period relating to the first wave, we have simplified the scenario considering only the national measures (i.e., *free* and *lockdown* classes). In the intermediate zone, we considered a somehow fictitious *summer* class that allows the model to gain the elasticity to include seasonal effects. Then, we considered a *light* class at the beginning of the second wave, followed by *yellow*, *orange,* and *red* classes corresponding to the containment measures actually included in the "colored" strategy (i.e. yellow, orange e red zones) adopted by the Italian government at reginal level. The *light* level is also identified to the *white* zone, given their similarities and considering that the regional *white* zone has been implemented only once in the considered time range.

In this study, we mainly focused on the *yellow*, *orange* and *red* classes to evaluate their differential impact and the effectiveness of their implementation. For the information on the confinement measures, we refer to the government decrees and the ordinances of the Ministry of Health [32], freely available from online resources [42,43].

2.4.1. Optimization

The free parameters to be optimized are in total 8: the 7 containment levels $F_{C,i}$ plus a scale factor S for the number of daily infections in the days before day zero. Actually, the time-marching evolution described by Equation (7) requires a set of initial values of $c(t)$corresponding to

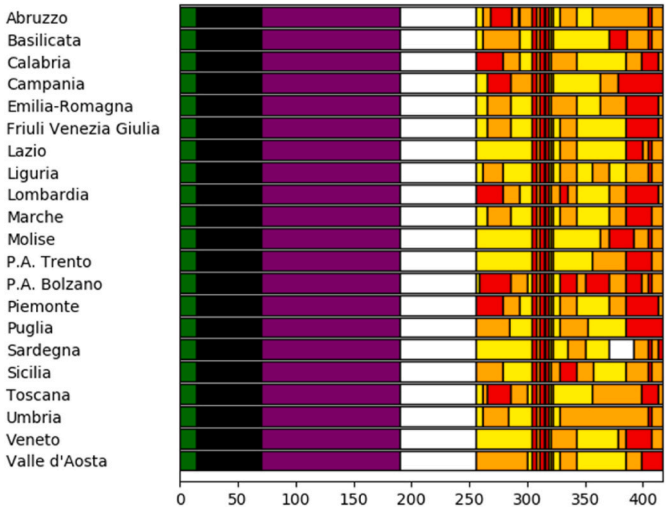

Fig. 1. Summary view of the calendar of confinement measures for the various Italian regions. The green region corresponds to the *free* zone, the black region corresponds to the *lockdown* period, the purple region corresponds to the *summer* period, the light region corresponds to the *light* zone; the yellow, orange and red regions correspond to the yellow, orange and red zone actually adopted by the Italian government at regional level. On the abscissa, the number of days since the initial reference day 2021-02-24.

time in the interval $[-a_2, 0]$. These starting values have been taken to follow the exponential growing behavior $c(t) = S{\cdot}e^{\lambda(t-t_0)}$ typical of the first wave where λ and $t_0$factors for each region have been separately evaluated in advance fitting the first part of the real confirmed cases using a classical least square method (Supplementary File - Supplementary Fig. 2).

The 8 free parameters were determined by minimizing the cost function:

$$\min_{F_i}\left(\int_0^T [\,c_{real}(t) - c_{simulated}(t \mid F_i)]^2\, dt\right) \tag{13}$$

where $c_{simulated}(t) = c(t)$ previously defined and $c_{real}(t)$ is the real number of daily infections at time t.

The range of data used in the optimization starts from the first day available in the public repository – 2020-02-24 – up to the 418-th day, which corresponds to the date 2021-04-16, freely available from Refs. [42,43].

The chosen optimization algorithm is *differential evolution* [44], a so-called metaheuristic method designed to search for global minima in a wide range of available parameters. The optimal parameters are searched for in intervals defined in our case between 0.05 and 10, reasonable values considering that these are ideal basic reproduction values and a scale factor around 1. Our software implementation is based on Python language (v 3.6.9) and takes advantage of the SciPy package (v 1.4.1).

2.5. Real data

Notwithstanding real data are publicly available [45], they are very sensitive since they strongly depend on the number of swabs carried out daily and on the presence of asymptomatic infected [10,17,46–51] as can be seen by comparing the number of the daily infections with the number of daily deaths in two significant Italian regions, Lazio and Lombardia (Supplementary File - Supplementary Fig. 3). Thus, we estimated the number of daily infections from the daily death cases $d(t)$ as:

$$c_{real}(t) = \frac{d(t-\delta_M)}{M(t)} \tag{14}$$

where $M(t)$ is the mortality trend and we assumed a temporal offset $\delta_M =$ 15 days. In addition, the trends are smoothened to avoid high frequencies of little significance to the model. We can calculate the average mortality starting from the mortality rates for the different population groups and considering that gradually the most fragile part of the population is (at least partially) protected (Supplementary File -Supplementary Fig. 4 left). Thus, we estimated the mortality trend $M(t)$as follows (Supplementary File - Supplementary Fig. 4 right):

$$M = \frac{\sum_i M_i \cdot S_i}{\sum_i S_i} \tag{15}$$

$$S_i = N_{P,i} - f_{VM}{\cdot}V_i(t-\delta_V) \tag{16}$$

where M_i is the mortality rate at the different age groups weighted with the number of unprotected individuals at that age group S_i and normalized with the total number of unprotected individuals. In order to estimate M_i, we used data available from Ref. [52]. Yet, $V_i(t-\delta_V)$ is a function describing the vaccinated people at time t for each age group, considering as vaccinated those that received the first dose at least from 20 days ($\delta_V = 20$); f_{VM} is the fraction of the vaccinated that are protected from serious evolution of the disease and fatal outcomes. We roughly assumed $f_{VM} = 95\%$ for the vaccines currently used in Italy.

Extrapolating the infections from the number of deaths using this mortality value, we obtain a curve that includes a greater number of infected individuals than those officially reported, with a curve fluctuating around 20–30% (again with reference to the second wave). This is therefore the quantity of undetected infected that we include in our data, which most likely matches the number of asymptomatic or paucisymptomatic cases [46].

3. Results

3.1. Model reliability in fitting the actual COVID-19 infection trend

To assess the quality of the model outcomes, in Fig. 2, by way of example, we provide the comparison between the real trend and the simulated trend of daily infections for the Emilia-Romagna region.

The trend of the first wave is reproduced very accurately, while the much more complex trend from the second wave onwards is reproduced satisfactorily, albeit with a more limited fidelity in relation to the individual fluctuations. The algorithm also manages to correctly ignore a small group of outlier's data around day 150, probably related to compensation of past inaccurate data. The corresponding table shows the F_C values relating to the various containment situations. We have seen how these values can be interpreted as R_0 if variant diffusion and decreasing of susceptible individuals is ignored. In the third column, we report $1.4{\cdot}F_C$ to consider the greater transmissibility of the English variant. In the first wave and in the first part of the second wave, it is more significant to consider $R_0 = F_C$, while in the last few weeks the other column that is more significant, i.e., $R_0 = 1.4{\cdot}F_C$, as the upper bound to be reduced considering the number of reduced susceptible individuals. The obtained results show values around 2 for the *free* situation, which fall well below the unit for the *lockdown* (considering in particular the absence of the English variant). The *summer* part is also characterized by a descending trend of the epidemic, which instead restarts with dramatic intensity, even if lower than the initial one, from the beginning of September (corresponding to the phase we marked as *light*). The *yellow* area proved to be unable to limit the epidemic even excluding the spread of the English variant, while the success of the *orange* level depends on the spread of the variant and on the ratio of susceptible population. The *red* zone, on the other hand, is always effective, and for this region it appears even more effective than the *lockdown* of the first wave.

The comparisons between real and simulated data for all the other regions are shown in Fig. 3.

In Fig. 4, we provided the plots of the optimized coefficients F_C (Fig. 4A) across the different regions and for different containment levels, along with their averaged values among the Italian regions (Fig. 4B) to easily visualize the comparison among these levels. The same plots are also provided for the corresponding rescaled factors $1.4\,F_C$ (Fig. 4C–D). The trends of optimized F_C coefficients give indications of the quality of containment, i.e., the *free* zone features a clear unstable behavior across the regions (always greater than 1), while the *lockdown* always guarantees decaying behaviors, remaining always below 1 (Fig. 4A); whilst the trends of the rescaled factor $1.4\,F_C$ allows to consider the upper bound of the reproduction number when the English variant is dominant and no reduction of susceptible individuals is considered (Fig. 4C–D).

Finally, in Fig. 5, the whole table of results is provided highlighting the values $F_C > 1$. Four values of the table were identified as unrealistic and marked using strikethrough. Among them, three cases correspond to *red* zone coefficients for Sardegna, Umbria, Liguria, where the *red* zone was used only on a few days so far. For this reason, the optimizer could not get accurate values for these numbers. The fourth case is the free value for Basilicata, too high and probably due to the very modest first wave for this region.

3.2. Model predictability of the optimal COVID-19 trend

The model developed, optimized, and validated can be used to

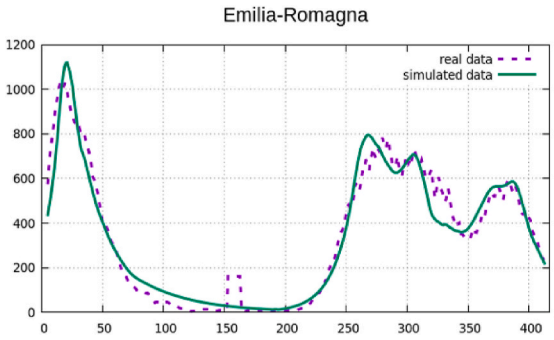

Confinement	F_C	$1.4 \cdot F_C$
Free	1.96	2.74
Lockdown	0.65	0.91
Summer	0.76	1.06
Light	1.84	2.57
Yellow	1.11	1.55
Orange	0.86	1.20
Red	0.52	0.73

Fig. 2. Real and simulated trends of daily infections for Emilia-Romagna. (Left) Comparison between the starting data and the simulated data of the temporal trends of the daily infections (normalized) for Emilia-Romagna. The simulated trends use the optimized parameters extracted from the differential evolution method correctly reached the convergence. (Right) The table shows the basic reproduction numbers corresponding to the different containment measures resulting from the optimization process for the considered region. Column $F_C$reports the values directly obtained, while column $1.4 \cdot F_C$ corresponds to the rescaled values including the greater contagiousness of the English variant. On the abscissa, the number of days since the initial reference day 2021-02-24.

reproduce trends in artificial conditions, e.g., considering alternative calendars of confinement measures. The zones' temporal sequence imposed by the "region coloring" mechanisms adopted in Italy were guided by the need to maintain the basic reproduction around unity and to avoid the saturation of hospital availability. This strategy strongly operates only when the spread of the virus is already high and is not able to significantly decrease the prevalence of the virus but only to contain it. At the beginning of the second wave, the number of new Italian daily infections largely exceeded 30,000 cases, with a probable underestimation due to the presence of asymptomatic individuals. Even considering the delay time between a containment action and its effect, it is clear that this is the result of a containment action implemented with considerable delay. Using our model, we tried to simulate, for the Lazio region example, the epidemic evolution starting from the second wave, assuming an initial anticipated containment action corresponding to the addition of two weeks of *red* zone, instead of *light* zone (Fig. 6). By comparing the effectiveness of the alternative and real closure calendar, we found that a timelier containment action, although limited to only two weeks, strongly affects the epidemic evolution trend. In terms of infections – integral of the curve – we obtained: 35,000 instead of 56,000 infections for the second wave of Lazio (Fig. 6). Thus, a more reactive containment strategy has a much higher cost-benefit return than a delayed strategy.

4. Discussion

4.1. Predictions of our model

In this study, we proposed an integro-differential model able to reproduce the wave-like dynamics of the COVID-19 epidemics in Italy since the beginning (February 24, 2021) up to April 16, 2021. Vaccination, virus variants, different confined strategies were included therein and the optimal model parameters were computed for each Italian region separately. Despite the regional variability, the poor accuracy of the starting data, the lack of repeating patterns, our model accurately reproduced the actual trend of the epidemic evolution (Figs. 2–3) as well as the different effectiveness of the containment measures adopted on a regional scale (Figs. 4–5). Moreover, we found that the ideal reproduction number R_0, strictly related to F_C, estimated by our model increases when relaxing the containment measures (Figs. 4–5). In particular, we observed how the *free* and *light* phases significantly differ from each other, demonstrating that even not too aggressive measures in the light zone have an important improvement effect (Fig. 4A). However, even the *light* zone showed a clear expansive effect and is therefore not suitable for the containment of the epidemic, regardless of the presence of the English variant (Fig. 4). Similarly, the *lockdown* phase presented a clear trend of epidemic contraction, even assuming the greater transmissibility of the English variant, however, not present in the actual lockdown period (Fig. 4B). The *summer* period showed values mostly lower than 1 considering the absence of the English variant, as actually happened (Fig. 4A). Although the results relative to *summer* are quite clear, we are not able from our analysis to give a causal correlation of the results in this phase which has several inextricably linked features (high temperatures, more effective sun exposure, change of social habits with more outdoor life, etc.) as well as a particular uniqueness given by coming after the long period of lockdown that has profoundly marked common social attitudes. As for the colored areas of the second phase, *yellow* is characterized by $F_C$around 1 in the absence of a variant (Fig. 4A), while it quite clearly exceeds the unity value considering the variant (Fig. 4B). In fact, as can be seen from Figs. 4–5, the ability of the *yellow* zone to contain the epidemic depends on the region in question, so it represents a rather risky mode of containment, although socially more manageable in the medium to long term. The effect of *orange* was significantly better and values around 1 were achieved only with the spread of the English variant (Fig. 4B). However, the only area capable of stopping the growth of the epidemic is the *red* area, even if the beneficial effects are lower than those of the March lockdown (Fig. 4). Even in full diffusion of the English variant, the *red* zone guarantees in most cases coefficients below unity (Fig. 5). Thus, the English variant plays a fundamental role in determining the effectiveness of the zones, and the consequent need to adopt more stringent zones. At the same time, the reduction on the number of susceptible individuals is also crucial, thus making even the first stage of vaccinations essential to cooperate with the confinement measure for obtaining a stable evolution. In fact, from equation (11), we can notice that the increase in the number of recovered cases and the vaccinated individuals leads to a reduction in the number of the susceptible individuals and, as a consequence from equation (9), a reduction in the reproduction number $R(t)$. For instance, starting with $F_S = 1$ and considering a yellow zone ($F_C = 0.93$ in Lazio) in the presence of the English variant ($F_V = 1.4$), we obtain $R = 1.3$. Then, considering a 25% reduction of the susceptible individuals ($F_S = 0.75$) due to the vaccinated and recovered individuals, R becomes again less than one ($R = 0.98$). It means that a limited number of vaccinated people (less than 25%, since we are considering that 25% is the total of vaccinated and recovered individuals) is potentially capable of inverting the effectiveness of a confinement level. Instead, if we consider less severe conditions, e.g., a *light* zone ($F_C = 1.41$ in Lazio) always in the presence of the English variant ($F_V = 1.4$), the F_S value required to stop the epidemy must be halved ($F_S = 0.496$ to obtain the same $R = 0.98$), meaning doubling the number of vaccinated or healed people. Conversely, if we consider the *free* condition zone ($F_C = 2.37$ in Lazio and $F_V = 1.4$), the F_S value required to stop the epidemy must be very low ($F_S = 0.29$ to obtain the same $R = 0.98$), meaning about 70% of vaccinated and recovered. In fact, with a value of $F_S = 0.75$, considering a *light* or *free* zone, we would have obtained $R = 1.4$ or $R = 2.5$. It means that, although vaccinations are expected to lead to a successfully handling of the epidemic, relaxing the confinements before reaching herd immunity must be considered with care and timely interventions, in order to ensure that the balance of the discussed factors teams up to produce

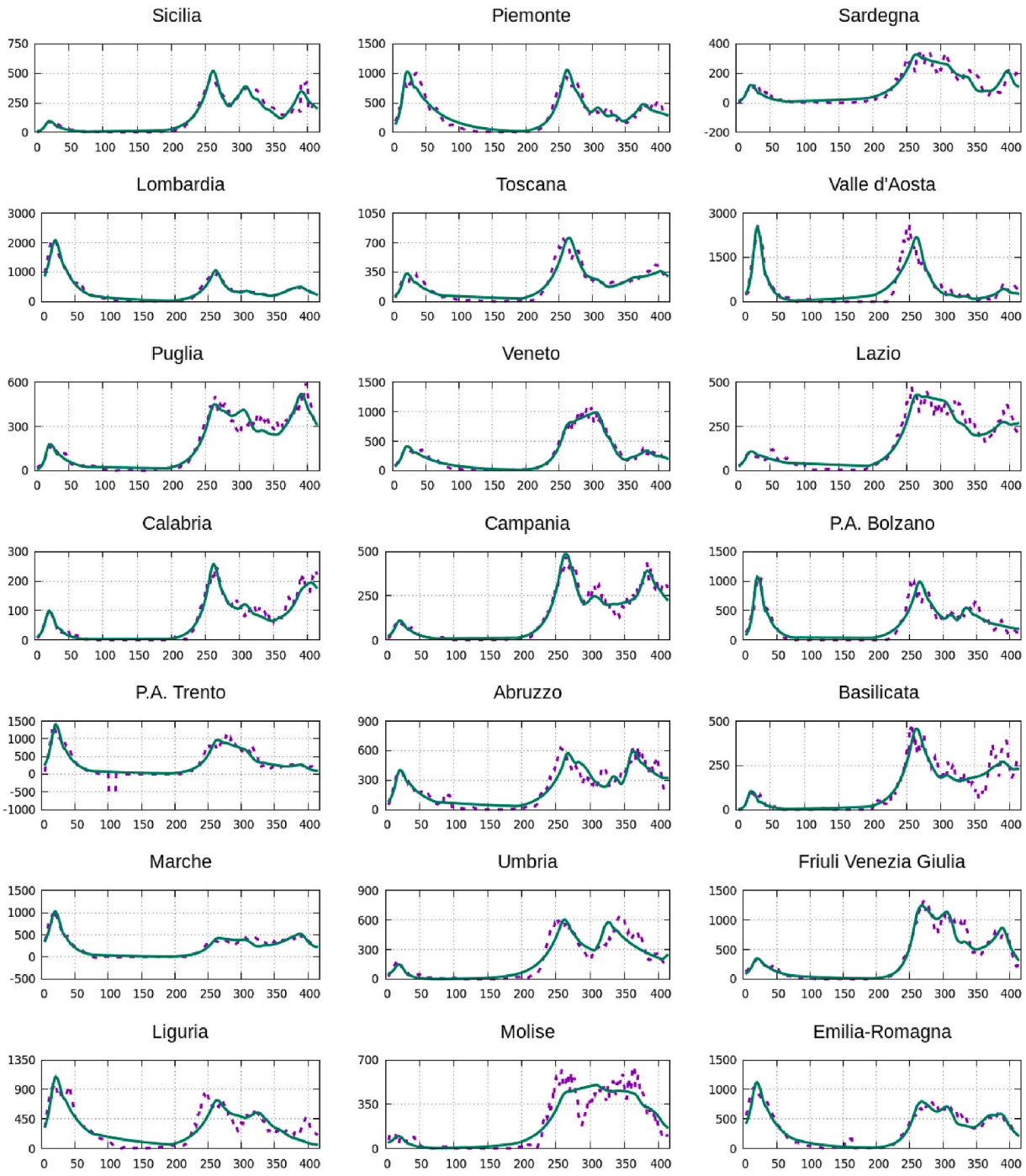

Fig. 3. Real and simulated trends of daily infections for Italian regions. Comparison between the starting data (solid line) and the simulated data (dashed line) of the temporal trends of the daily infections (normalized) for different Italian regions. The simulated trends use the optimized parameters extracted from the differential evolution method correctly reached the convergence. On the abscissa, the number of days since the initial reference day 2021-02-24.

favorable outcomes.

4.2. Comparison with other models

In Table 1 the main features of the most promising models developed to portray the dynamic spread of the COVID-19 pandemic are provided. Among the simplest models, Bhardwaj et al. [53] proposed a logistic model that gives insights only into the cumulative number of infections, and not into counts associated with other compartments like deaths and/or recoveries. Moreover, it does not account for other crucial factors for tracing COVID-19 pandemic, such as the incubation period, the asymptomatic infectives, or the effect of confinements measures.

Among SIR-based models, Fiscon et al. [6] proposed an extension of the SIR model that explicitly considers asymptomatic infectives, and optimized the model parameters through a best-fitting approach that locally minimizes the sum of square error between the observed and estimated infectives. However, the lack of containment measures does not allow to adequately follow the realistic behaviours of data. Wang et al. [25] extended the standard SIR model by incorporating time-varying isolation measures (e.g., government-level macro isolation and community-level micro inspection measures). This model is valuable for its attempt to put together different ingredients of the epidemic

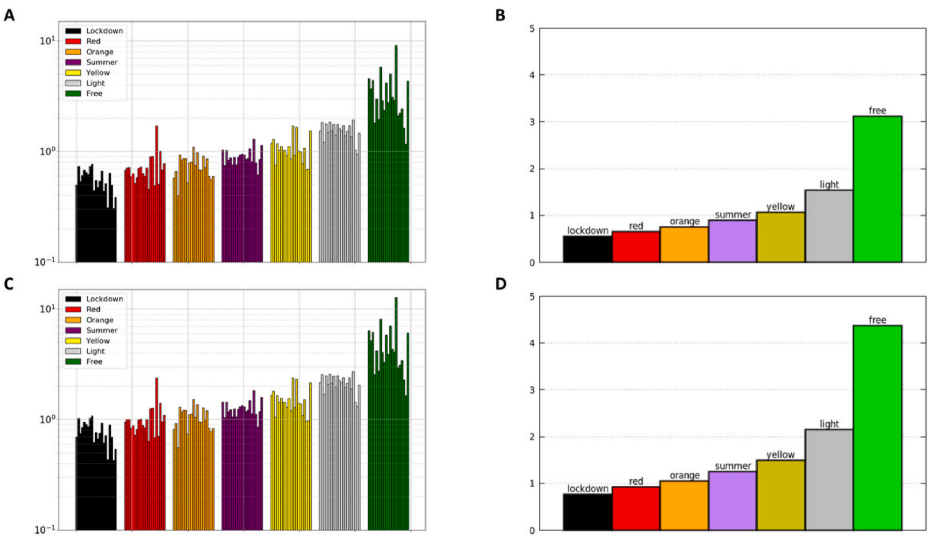

Fig. 4. Representation of the optimized parameters F_C (A–B) and the rescaled $1.4\,F_C$ values (C–D) for different containment levels across the Italian regions. (A) Bar plot of the values of the optimized parameters F_C corresponding to the different containment levels (i.e., different colors) across the Italian regions. Log scale is used on y-axis. **(B)** Bar plot of the average values among the Italian regions of the optimized parameters F_C. Unrealistic values have been neglected to perform the averages. **(C-D)** The same bar plots of panel A and C for the rescaled factor of $1.4\,F_C$ to consider the greater contagiousness of the English variant.

Region	free	lockdown	summer	light	yellow	orange	red
Sicilia	4.56	0.50	1.03	1.54	1.19	0.58	0.68
Piemonte	3.70	0.73	0.75	1.83	1.29	0.66	0.71
Sardegna	4.40	0.53	1.03	1.21	0.75	0.40	~~0.72~~
Lombardia	1.82	0.61	0.84	1.77	1.18	0.93	0.60
Toscana	2.99	0.68	0.88	1.49	1.03	0.84	0.63
Emilia-Romagna	1.96	0.65	0.76	1.84	1.11	0.86	0.52
Puglia	5.82	0.62	0.89	1.53	1.02	0.87	0.58
Veneto	2.89	0.74	0.76	1.76	1.03	0.53	0.71
Lazio	2.37	0.77	0.89	1.41	0.93	0.79	0.72
Calabria	4.15	0.44	0.93	1.77	1.10	0.80	0.63
Campania	2.79	0.55	0.95	1.61	0.86	1.09	0.60
P.A. Bolzano	5.01	0.48	0.93	1.54	1.70	0.75	0.71
P.A. Trento	3.10	0.54	0.85	1.71	0.92	0.98	0.46
Abruzzo	2.91	0.66	0.87	1.40	1.66	0.68	0.90
Basilicata	~~9.11~~	0.44	1.06	1.53	1.01	0.68	0.91
Marche	2.11	0.51	0.81	1.71	0.99	0.91	0.49
Umbria	2.22	0.31	1.30	1.36	0.78	0.72	~~1.70~~
Friuli Venezia Giulia	2.44	0.64	0.79	1.93	1.08	0.86	0.51
Liguria	1.63	0.49	0.61	1.03	0.69	0.59	~~1.01~~
Molise	1.17	0.31	0.85	0.94	0.70	0.56	0.68
Valle d'Aosta	4.33	0.39	1.14	1.46	1.54	0.60	0.78

Fig. 5. Optimized values for containment factors F_C for different levels and different regions. Unstable factors (greater than 1) are highlighted using gray background. Unrealistic values are marked using strikethrough.

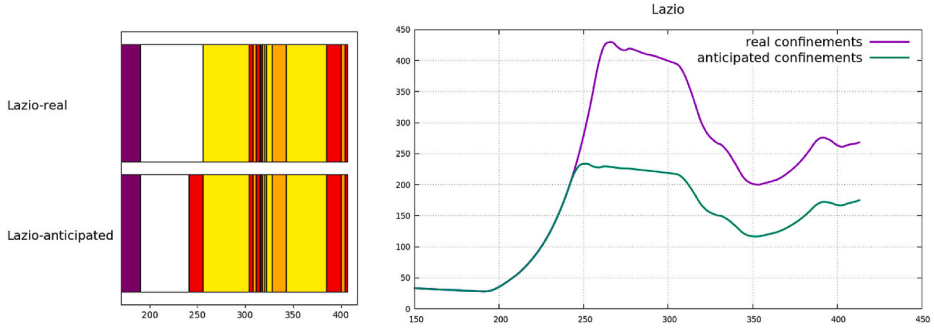

Fig. 6. Artificial daily infections trends in Lazio. (Left) Visualization of the confinement calendars of Lazio from the second wave onwards in comparison between real confinement and anticipated confinement. (Right) Trends in daily infections in Lazio as modeled according to the confinement calendars presented in the figure on the left.

Table 1
Overview of compared models.

Model	Model type	Estimation of optimal parameters	Parameter(s)						
			SOI	Asymptomatic infectives	Incubation period	Virus variants	Vaccine effect	Mobility factors	Containment measures
Bhardwaj et al., 2020 [53]	Logistic model	Least-squares regression and Markov chain-Monte Carlo							
Fiscon et al., 2021 [6]	Extension of standard SIR model	Best-fit approach to locally minimize SSE		✓					
Wang et al., 2020 [25]	Extension of standard SIR model	Markov chain-Monte Carlo							✓
Giordano et al., 2021 [26]	Extension of standard SIR model	Best-fit approach to locally minimize SSE	✓	✓					✓
Bhaduri et al., 2020 [27]	Extension of standard SEIR model	Markov chain-Monte Carlo		✓	✓				
Hao et al., 2020 [28]	Extension of standard SEIR model	Markov chain-Monte Carlo	✓	✓	✓				
Flaxman et al., 2020 [30]	Bayesian semi-mechanistic model	Hamiltonian Markov chain-Monte Carlo							✓
Santamaria et al., 2020 [31]	Linear model	Regression best-fit approach						✓	✓
Salvadore et al., 2021	Integro-differential model	Differential evolution algorithm		✓	✓	✓	✓		✓

SOI: different Severity Of Illness.
SSE: Sum of Square Errors.

evolution, but is applied only to the period of the so-called first wave of the virus and has some weaknesses: it does not consider the existence of asymptomatic subjects and of a period of incubation of the virus; it includes the transmission rate modifier due to the different confinement measures as externally imposed data and is therefore difficult to use in more complex contexts with unpredictable confinement effects (e.g., the period of the second pandemic wave). The results for R(t) of the first Italian wave are however compatible with those found in our analysis. Giordano et al. [26] proposed a SIR-type model that has been applied to the first Italian wave and the authors outlined possible scenarios of countermeasure implementation, predicting that restrictive social-distancing measures were needed to be combined with widespread testing and contact tracing to stop the epidemic. However, the interpretation of reduced transmission rates due to confinement measurements is not straightforward to extract, especially considering a second wave complex scenario. In addition, the model does not account for a possible latency between exposure to the virus and onset of infectiousness. Hao et al., 2020 [28] proposed a Susceptible, Exposed, Infected and Removed (SEIR) model which, besides the incubation period, accounts for the infectiousness of asymptomatic and pre-symptomatic individuals in the population, and explicitly models population movement and time varying ascertainment rates. The model is only applied to the Wuhan (first) wave where the confinement measures can be easily identified. Bhaduri et al. [27] proposed another extension of standard SEIR model accounting for asymptomatic infectives, containment measures but also for the possible effect of misclassifications due to imperfect testing (false negative rate - infected people who are tested but reported as negative). The model has been applied to the Indian epidemic behaviour up to the 2020 summer. For both the above-mentioned SEIR-type models [27,28], the estimation of model parameters is based on Markov chain-Monte Carlo methods. For these models, due to the different context of application, a direct comparison with our results is not possible.

Among more complex models, Flaxman et al. [30] proposed a Bayesian semi-mechanistic model that relies on observed deaths data and calculates backwards to infer the true number of infections, as well as the time-varying reproduction number R(t). The primary objective of the model is to assess the effect of non-pharmaceutical interventions on different European countries. The results refer to 11 European countries and show a transmission reduction capacity achieved by lockdown around 80%. This value is very similar to the mean reduction factor across the Italian regions as obtained in the study presented here (F_C is reduced from about 3 considering *free* condition to about 0.6 in *lockdown*). In this work, the authors showed that evaluating the effectiveness of the containment measurements is more challenging when considering specific interventions (e.g., public events' limitations or school closure) than when considering global intervention (e.g., lockdown). This confirms the reasonableness of our approach, which considers the confinements measures grouped in the *colored* zones. A real quantitative comparison of the results of this model with those of our model is not possible for confinements different from the lockdown. However, we observed that the colored zones implemented in Italy led to a significant reduction in transmissibility, with the red zone effectiveness similar to the lockdown one. This is consistent with what we found in Ref. [30] where the authors showed that the single intervention has a very modest reductive capacity on transmission (e.g., 20% for school lockdown). Santamaria et al. [31] proposed a model based on a mobility indicator obtained from anonymized travel data, with the aim of correlating different containment measures – extracted from the Oxford Covid-19 Government Response Tracker OxCGRT (Hale et al. [54]) – with mobility data. However, it has been shown that the effects of containment on mobility cannot be directly translated into effects on the transmissibility factor, as they ignore the effect of distancing rules (making movements less dangerous).

Despite the undoubtedly validity of the models presented in Refs. [30,31], they are directly oriented to the evaluation of containment measures using data for a specific stage of the epidemic evolution, and disregard other crucial factors such as the effect of vaccination or the effect of the virus variants. For this reason, the model proposed in this study emerges as more comprehensive.

5. Conclusions

Although the COVID-19 pandemic has been the focus of the attention of much of the world's population for several months, many questions still remain open. Main concerns rise about the effectiveness of the strategies implemented by governments to limit the virus spread. In particular, in the European context, the strategy of "coexistence with the virus" has led to the implementation of confinement measures with the declared aim of achieving the best compromise between the restriction of personal freedoms and economic and health consequences. Yet, an evaluation of the effectiveness of the different measures is difficult due to the large number of involved parameters, the limited reliability of the measured data, and the scarce amount of data repeated under similar conditions. However, the Italian situation is a significant test case, since a strategic plan with regionally differentiated scenarios was introduced, especially from the so-called second wave onwards, with confinement levels and attribution criteria quite uniform across the Italian regions.

Having shown the possibility of attributing significant numerical trends corresponding to the different levels of confinement, we proposed some reflections on the strategies adopted in Italy and on the quality of the response given, within the framework of the so-called "coexistence with the virus" and the methods used to implement it. It emerges that the delay in taking the second wave seriously, led a very high load-bearing in the daily contagion curve and the subsequent setting to avoid the explosion of infections – maintaining a constant level on average –maintained this high average. More reactive criteria at the start of the second wave would have allowed to limit the peak at a very low cost in terms of restrictive measures. Leaving the subsequent trend unchanged, this would have led to a much lower number of total infections.

The actual predictive capabilities of our model as well as simple procedures for fixing model parameters not subject to optimization may be the subject of subsequent elaborations.

Data availability

As for the information on the confinement measures, we refer to the government decrees and the ordinances of the Italian Ministry of Health [32], already partially accessible in a schematic way in freely available online resources [42,43].

Declaration of competing interest

The authors declare that there are no competing interests.

Acknowledgements

This work was supported by PRIN 2017 - Settore ERC LS2 - Codice Progetto 20178L3P38. The authors gratefully acknowledge the valuable assistance of Tony Brennan for language editing.

Appendix A. Supplementary data

Supplementary data to this article can be found online at https://doi.org/10.1016/j.compbiomed.2021.105013.

Author contributions

FS and PP: concept and design. FS developed the model and performed the simulations. All authors contributed to data analysis and interpretation, review, and approval of the final manuscript.

References

[1] J. Zheng, SARS-CoV-2: an emerging coronavirus that causes a global threat, Int. J. Biol. Sci. 16 (2020) 1678–1685.
[2] D. Wrapp, et al., Cryo-EM structure of the 2019-nCoV spike in the prefusion conformation, Science 367 (2020) 1260–1263.
[3] J.F.-W. Chan, et al., Genomic characterization of the 2019 novel human-pathogenic coronavirus isolated from a patient with atypical pneumonia after visiting Wuhan, Emerg. Microb. Infect. 9 (2020) 221–236.
[4] R. Lu, et al., Genomic characterisation and epidemiology of 2019 novel coronavirus: implications for virus origins and receptor binding, Lancet 395 (2020) 565–574.
[5] B. Hu, H. Guo, P. Zhou, Z.-L. Shi, Characteristics of SARS-CoV-2 and COVID-19, Nat. Rev. Microbiol. 19 (2021) 141–154.
[6] G. Fiscon, F. Salvadore, V. Guarrasi, A.R. Garbuglia, P. Paci, Assessing the impact of data-driven limitations on tracing and forecasting the outbreak dynamics of COVID-19, Comput. Biol. Med. 135 (2021), 104657.
[7] Y. Wang, Y. Wang, Y. Chen, Q. Qin, Unique epidemiological and clinical features of the emerging 2019 novel coronavirus pneumonia (COVID-19) implicate special control measures, J. Med. Virol. 92 (2020) 568–576.
[8] Y. Bai, et al., Presumed asymptomatic carrier transmission of COVID-19, J. Am. Med. Assoc. 323 (2020) 1406–1407.
[9] A. Kimball, et al., Asymptomatic and Presymptomatic SARS-CoV-2 infections in residents of a long-term care skilled nursing facility - King county, Washington, March 2020, MMWR Morb. Mortal. Wkly. Rep. 69 (2020) 377–381.
[10] R. Li, et al., Substantial undocumented infection facilitates the rapid dissemination of novel coronavirus (SARS-CoV-2), Science 368 (2020) 489–493.
[11] D.P. Oran, E.J. Topol, Prevalence of asymptomatic SARS-CoV-2 infection, Ann. Intern. Med. 173 (2020) 362–367.
[12] I. Arevalo-Rodriguez, et al., False-negative results of initial RT-PCR assays for COVID-19: a systematic review, PLoS One 15 (2020), e0242958.
[13] S. Gandini, et al., A cross-sectional and prospective cohort study of the role of schools in the SARS-CoV-2 second wave in Italy, Lancet Reg. Health - Eur. 5 (2021), 100092.
[14] W.O. Kermack, A.G. McKendrick, G.T. Walker, A contribution to the mathematical theory of epidemics, Proc. R. Soc. Lond. - Ser. A Contain. Pap. a Math. Phys. Character 115 (1927) 700–721.
[15] C. Anastassopoulou, L. Russo, A. Tsakris, C. Siettos, Data-based analysis, modelling and forecasting of the COVID-19 outbreak, PLoS One 15 (2020), e0230405.
[16] D. Fanelli, F. Piazza, Analysis and forecast of COVID-19 spreading in China, Italy and France, Chaos, Solit. Fractals 134 (2020), 109761.
[17] G. Gaeta, G. Gaeta, A simple SIR model with a large set of asymptomatic infectives, Math. Eng. 3 (2021) 1–39.
[18] J.T. Wu, et al., Estimating clinical severity of COVID-19 from the transmission dynamics in Wuhan, China, Nat. Med. 26 (2020) 506–510.
[19] Q. Lin, et al., A conceptual model for the coronavirus disease 2019 (COVID-19) outbreak in Wuhan, China with individual reaction and governmental action, Int. J. Infect. Dis. 93 (2020) 211–216.
[20] J. Chu, A statistical analysis of the novel coronavirus (COVID-19) in Italy and Spain, PLoS One 16 (2021), e0249037.
[21] A. Moussaoui, P. Auger, Prediction of confinement effects on the number of Covid-19 outbreak in Algeria, Math. Model Nat. Phenom. 15 (2020) 37.
[22] F. Casella, Can the COVID-19 epidemic be controlled on the basis of daily test reports? IEEE Control Syst. Lett. 5 (2021) 1079–1084.
[23] M. Renardy, M. Eisenberg, D. Kirschner, Predicting the second wave of COVID-19 in Washtenaw county, MI, J. Theor. Biol. 507 (2020), 110461.
[24] B. Ghanbari, On forecasting the spread of the COVID-19 in Iran: the second wave, Chaos, Solit. Fractals 140 (2020), 110176.
[25] J. Wangping, et al., Extended SIR prediction of the epidemics trend of COVID-19 in Italy and compared with Hunan, China, Front. Med. 7 (2020) 169.
[26] G. Giordano, et al., Modelling the COVID-19 epidemic and implementation of population-wide interventions in Italy, Nat. Med. 26 (2020) 855–860.
[27] R. Bhaduri, et al., EXTENDING the SUSCEPTIBLE-EXPOSED-INFECTED-REMOVED (SEIR) MODEL to HANDLE the HIGH faLSE nEGATIVE RATE and syMPTOM-BASED ADMINISTRATION of COVID-19 DIAGNOSTIC TESTS: SEIR-Fansy, vol. 9, 2020, p. 20200238, 24, https://www.medrxiv.org/content/10.1101/2020.09.24.20200238v1 (2020) doi:10.1101/2020.09.24.20200238.
[28] X. Hao, et al., Reconstruction of the full transmission dynamics of COVID-19 in Wuhan, Nature 584 (2020) 420–424.
[29] S.A. Lauer, et al., The incubation period of coronavirus disease 2019 (COVID-19) from publicly reported confirmed cases: estimation and application, Ann. Intern. Med. 172 (2020) 577–582.
[30] S. Flaxman, et al., Estimating the effects of non-pharmaceutical interventions on COVID-19 in Europe, Nature 584 (2020) 257–261.
[31] C. Santamaria, et al., Measuring the impact of COVID-19 confinement measures on human mobility using mobile positioning data. A European regional analysis, Saf. Sci. 132 (2020), 104925.
[32] Ministero della Salute. http://www.salute.gov.it/portale/nuovocoronavirus/archivioNormativaNuovoCoronavirus.jsp.
[33] J. Wallinga, M. Lipsitch, How generation intervals shape the relationship between growth rates and reproductive numbers, Proc. R. Soc. B Biol. Sci. 274 (2007) 599–604.
[34] J. Ma, Estimating epidemic exponential growth rate and basic reproduction number, Infect. Dis. Model. 5 (2020) 129–141.
[35] Infection. European Centre for disease Prevention and control https://www.ecdc.europa.eu/en/covid-19/latest-evidence/infection.
[36] Public Health England, Public Health England Vaccine Effectiveness Report March 2021, 2021, p. 11.
[37] European Centre for Disease Prevention and Control, Rapid Increase of a SARS-CoV-2 Variant with Multiple Spike Protein Mutations Observed in the United Kingdom, 2021, p. 13.

[38] Istituto Superiore di Sanita, Prevalenza delle varianti VOC (variant of concern), in: Italia: lineage B.1.1.7, P.1, P.2,lineage B.1.351, lineage B.1.525 (Indagine del 18/3/2021), 2021.
[39] Istituto Superiore di Sanita, Prevalenza delle varianti VOC 202012/01 (lineage B.1.1.7), P.1, e 501.V2 (lineage B.1.351) in Italia (Indagine del 18 febbraio 2021), 2021.
[40] N.G. Davies, et al., Estimated transmissibility and impact of SARS-CoV-2 lineage B.1.1.7 in England, Science 372 (2021).
[41] Istituto Superiore di Sanità, Speciale COVID-19 - Varianti del virus, 2021.
[42] Gestione Della Pandemia Di COVID-19 in Italia, 2020, November 19. https://it.wikipedia.org/wiki/Gestione_della_pandemia_di_COVID-19_in_Italia.
[43] Asusual Lab. Covidzone, 2021. https://covidzone.info/.
[44] R. Storn, K. Price, Differential evolution – a simple and efficient Heuristic for global optimization over continuous spaces, J. Global Optim. 11 (1997) 341–359.
[45] Presidenza del Consiglio dei Ministri - Dipartimento della Protezione Civile, Dati COVID-19 Italia, 2021. https://github.com/pcm-dpc/COVID-19.
[46] E. Lavezzo, et al., Suppression of a SARS-CoV-2 outbreak in the Italian municipality of Vo, Nature 584 (2020) 425–429.
[47] J. Lourenço, R. Paton, C. Thompson, P. Klenerman, S. Gupta, Fundamental principles of epidemic spread highlight the immediate need for large-scale serological surveys to assess the stage of the SARS-CoV-2 epidemic, medRxiv 2020 24 (2020), 20042291, https://doi.org/10.1101/2020.03.24.20042291, 03.
[48] S. Flaxman, et al., Estimating the effects of non-pharmaceutical interventions on COVID-19 in Europe, Nature 584 (2020) 257–261.
[49] S.W. Park, D.M. Cornforth, J. Dushoff, J.S. Weitz, The time scale of asymptomatic transmission affects estimates of epidemic potential in the COVID-19 outbreak, medRxiv (2020), https://doi.org/10.1101/2020.03.09.20033514.
[50] Y. Yu, et al., COVID-19 asymptomatic infection estimation, medRxiv 2020 19 (2020), 20068072, https://doi.org/10.1101/2020.04.19.20068072, 04.
[51] COVID-19. Imperial College London http://www.imperial.ac.uk/medicine/departments/school-public-health/infectious-disease-epidemiology/mrc-global-infectious-disease-analysis/covid-19/.
[52] Il tasso di mortalità per fascia d'età | TRT Italiano. https://www.trt.net.tr/italiano/photogallery/infografica/il-tasso-di-mortalita-per-fascia-d-eta.
[53] R.A. Bhardwaj, Predictive model for the evolution of COVID-19, Trans. Indian Natl. Acad. Eng. 5 (2020) 133–140.
[54] T. Hale, et al., A global panel database of pandemic policies (Oxford COVID-19 Government Response Tracker), Nat. Hum. Behav. 5 (2021) 529–538.